ELSEVIER

Contents lists available at ScienceDirect

Journal of Alloys and Compounds

journal homepage: www.elsevier.com/locate/jalcom





Exploiting mechanochemical activation and molten-salt-assisted reduction-diffusion approach in bottom-up synthesis of Sm₂Fe₁₇N₃

Rambabu Kuchi ^{a,*}, Deborah Schlagel ^a, Thomas A. Seymour-Cozzini ^b, Julia V. Zaikina ^b, Ihor Z. Hlova ^a

- a Critical Materials Innovation Hub, Ames National Laboratory, US Department of Energy, Iowa State University, Ames, IA 50011, USA
- ^b Department of Chemistry, Iowa State University, Ames, IA 50011, USA

ARTICLE INFO

Keywords: Sm₂Fe₁₇N₃ powders CaCl₂ molten salt Reduction-diffusion Mechanochemical Spark-plasma sintering

ABSTRACT

 $Sm_2Fe_{17}N_3$ powders were prepared by a novel molten-salt mechanochemically assisted reduction-diffusion (RD) approach. $CaCl_2$, plays a critical role during mechanochemical processing as a dispersant, facilitating the RD process by dissolving the precursors in a molten flux and further assisting during the washing step by efficient removal of by-products thus minimizing the surface oxidation of $Sm_2Fe_{17}N_3$ powder particles. Various milling times and RD temperatures were examined, and synthesis conditions were optimized to achieve pure-phase $Sm_2Fe_{17}N_3$ powders with low aggregation of magnetic particles. Powders synthesized at 950 °C RD exhibited the highest hard-magnetic properties: coercivity H_c of 13.5 kOe, and maximum energy product $(BH)_{max}$ of 19.4 MGOe. This was attributed to the formation of fine single-phase $Sm_2Fe_{17}N_3$ particles as well as minimal oxidation of particle surface. Furthermore, by densifying the $Sm_2Fe_{17}N_3$ powders with high-pressure spark plasma sintering, a bulk magnet with $(BH)_{max}$ of 16.5 MGOe and a relative density of 86 % was produced indicating that the obtained $Sm_2Fe_{17}N_3$ powders had low oxygen content.

1. Introduction

The improvement of the hard-magnetic properties in permanent magnets represents a significant area of research, given the widespread use of electrical motors and generators in various industries, especially in electric vehicles and wind turbines [1-4]. Nd₂Fe₁₄B-based magnets, which are currently widely utilized, have a low Curie temperature (~312 °C) and reduced performance at high temperatures [5]. Sm₂Fe₁₇N₃ exhibits a higher Curie temperature (~475 °C) and excellent hard-magnetic properties as a powder but is difficult to sinter due to the decomposition of Sm₂Fe₁₇N₃ to SmN, Fe, and N₂ at elevated temperatures of around 620 °C [6-8]. Nevertheless, when consolidation is conducted well below its decomposition temperature, the resultant sintered magnet exhibits a significant reduction in its magnetic properties [9]. This is attributed to the precipitation of fine α -Fe at the sintered interface, which occurs due to a redox reaction between the surface iron oxide film and the $Sm_2Fe_{17}N_3$ matrix: $Sm_2Fe_{17}N_3 + Fe_2O_3 \rightarrow$ $Sm_2O_3 + 19Fe + (3 N)$.

To overcome this obstacle, considerable effort has been focused on developing methods for producing high-performance $Sm_2Fe_{17}N_3$

powders with low oxygen content. The traditional method of preparing $\rm Sm_2Fe_{17}N_3$ powders involves melting Sm and Fe metals with rapid quenching, followed by nitridation, and the resultant coarse powder is pulverized by ball milling [10–12]. These methods require high purity metals and prove to be laborious in execution. Additionally, the obtained fine powders are susceptible to oxidation due to high surface area, defects, and irregular particle shapes generated during processing [13,14]. Therefore, a more direct method of producing fine $\rm Sm_2Fe_{17}N_3$ powders with high magnetic properties is needed.

Co-precipitation combined with the reduction-diffusion (RD) is a commonly used wet-chemical bottom-up approach to prepare fine $Sm_2Fe_{17}N_3$ powders directly [5,15,16]. The obtained powders exhibit high coercivities of more than 20 kOe, but this process utilizes co-precipitated precursors which are produced when evaporating large amounts of solutions, thus it is not very practical for mass production. One such example is reported by J. Zheng et al., when the ultrasonic spray pyrolysis-hydrogen reduction with subsequent RD and nitridation are employed to prepare fine $Sm_2Fe_{17}N_3$ powders [17]. These fine powders exhibit a coercivity of 14.7 kOe and, based on XRD analysis, do not show any impurity phases, except for a significant oxygen

E-mail address: rkuchi@ameslab.gov (R. Kuchi).

^{*} Corresponding author.

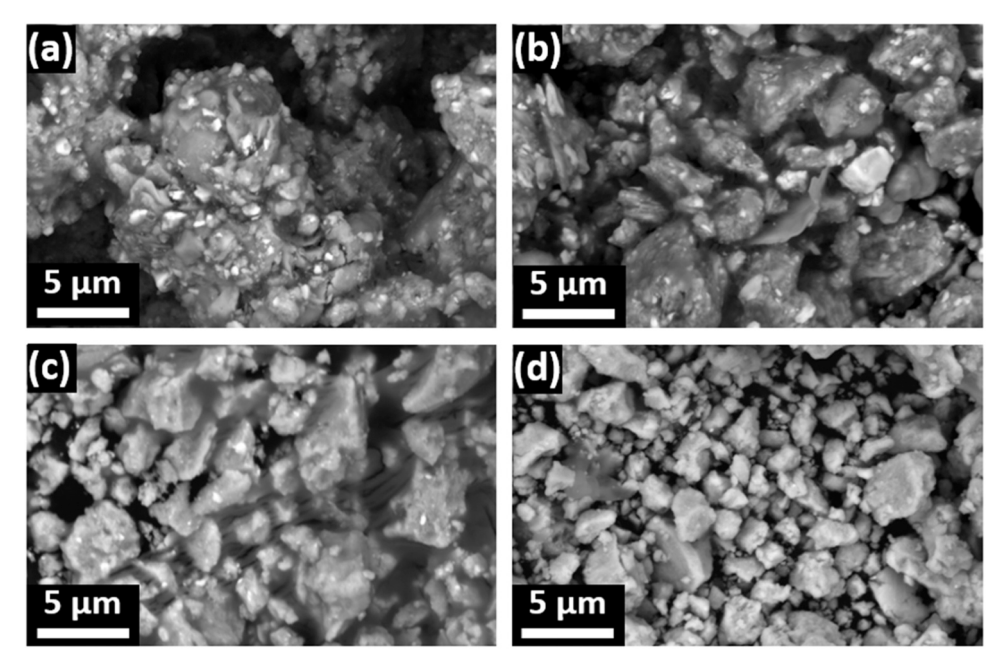


Fig. 1. BSE-SEM images of the precursor powders obtained by milling for different times: (a) 1 h, (b) 3 h, (c) 6 h, and (d) 10 h.

contamination (\sim 8 wt%), which can be attributed to the washing of powders with fine particle size. J. Lee et al. introduced a one-pot synthesis for production of ultrafine $\rm Sm_2Fe_{17}N_3$ nanoparticles with an average size of 300–400 nm. However, this method yielded powders with a modest maximum magnetic energy product (BH)_{max} of 13.9 MGOe [18]. All described methods involve multiple-step procedures, posing difficulties in controlling the final particle size and oxygen content, and making the production of sintered magnets challenging.

Recently, S. Sato et al. prepared an anisotropic Sm-Fe-N magnetic powder and its sintered magnets using the RD process and a low-melting eutectic LiCl-CaCl₂ [19]. Near single-phase Sm₁Fe₇ alloy powder was obtained using this approach, which enabled the reduction to occur below the melting temperature of Ca (T_{melt} = 842 $^{\circ}\text{C}$). However, upon sintering the obtained bulk magnet possessed inferior hard magnetic properties ($BH_{max} = 6.1$ MGOe, relative density of 86.8 %). Nevertheless, this approach suggests the feasibility of obtaining pure Sm₂Fe₁₇N₃ alloy powders using CaCl2 as a molten salt during high-temperature reduction-diffusion process. In this study, we utilized CaCl₂ as a flux during RD to prepare low-oxygen Sm₂Fe₁₇N₃ powders, which are crucial for bulk magnet fabrication, maintaining the same level of hard-magnetic performance as was observed in powders. The developed process involves mechanochemical activation of precursors by milling with CaCl2, followed by Ca-assisted RD, washing, nitrogenation, and finally by spark plasma sintering (SPS). Introduction of CaCl₂ allows to decrease the RD reaction temperature due to its lower melting point (T_melt CaCl $_2 = 772~^{\circ}\text{C}$) compared to Ca (T_melt Ca = 842 $^{\circ}\text{C}$). The molten $\mbox{\sc CaCl}_2$ serves as a liquid flux in which Ca dissolves and diffuses to reduce Sm₂O₃. As-formed Sm metal dissolves in CaCl₂ flux and diffuses to react with Fe particles, thereby completing RD by formation the Sm-Fe alloy. The commonly used deionized water (DIW) washing step applied after the reduction process effectively removed impurities and produced high-quality $Sm_2Fe_{17}N_3$ powder. In addition to utilizing $CaCl_2$ as a dispersant agent during the mechanochemical activation of precursors and as a molten salt flux, its high solubility in water significantly reduces washing time. This, in turn, results in minimal oxidation of the final powder particles. Thus, our proposed approach produces low-oxygen Sm₂Fe₁₇N₃ powders with high values of coercivity, saturation magnetization, and maximum energy product [(BH)_{max}] which is beneficial during consolidation into a bulk magnet.

2. Experimental procedure

The starting precursors – Sm₂O₃, Fe, and CaCl₂ – were procured from Sigma-Aldrich. To eliminate absorbed moisture, Sm₂O₃ was annealed at 800 °C for 12 h. To obtain anhydrous compound, CaCl2 was annealed with NH₄Cl in Ar flow at 350 °C for 4 h. The Sm₂Fe₁₇N₃ powder particles were prepared by mechanochemical milling of precursors followed by the molten salt assisted RD process. Briefly, the starting precursors, including Sm₂O₃, Fe and CaCl₂, were ball milled for a duration ranging from 1 to 10 h. Thereafter, the milled powder was mixed with Cagranules and annealed at 800 to 1000 °C for 1 h under Helium (He) gas. The RD powder was crushed in mortar to produce a coarse powder, which was then subjected to nitriding in an atmosphere consisting of a mixture of gasses comprised of NH₃-H₂ (1:2 vol/vol) at a temperature of 420 °C for 1 h. Afterward, the powder was annealed in an H₂ atmosphere to adjust the nitrogen content, followed by a 1 h annealing in an Ar atmosphere to remove any absorbed hydrogen from the Sm₂Fe₁₇N₃ [20]. Finally, the removal of the by-products from nitridated powders was carried out by washing step. For this purpose, we utilized washing with deionized (DI) water while sonicating. Then, powder was rinsed with acetone to remove any traces of water and dried under a vacuum to obtain the final magnetic powder used for consolidation. To produce bulk magnets, the obtained powders were placed into a 5 mm diameter cylindrical die made of tungsten carbide (WC) within an Ar atmosphere glovebox to avoid oxidation. Subsequently, the die was positioned in the chamber of a Spark Plasma Sintering (SPS) system (Dr. Sinter Lab Jr. SPS-211Lx 247, Sumitomo Mining Co., Ltd.). The SPS chamber was evacuated and backfilled with Ar gas pressure less than 0.5 Pa. Sintering was performed by applying a uniaxial compressive pressure of 750 MPa at a temperature of 420 $^{\circ}\text{C}$ for 5 min

X-ray diffraction (XRD, PAN Analytical, USA) using Cu K α radiation was utilized to assess the phase and crystal structure of the samples. The field emission scanning electron microscopy (FE-SEM, Teneo LoVac, FEI, USA) was employed to examine the particle morphology and size, chemical composition, and microstructure. A vibrating sample magnetometer (PPMS-Dynacool, Quantum Design, USA) was utilized to measure the magnetic properties.

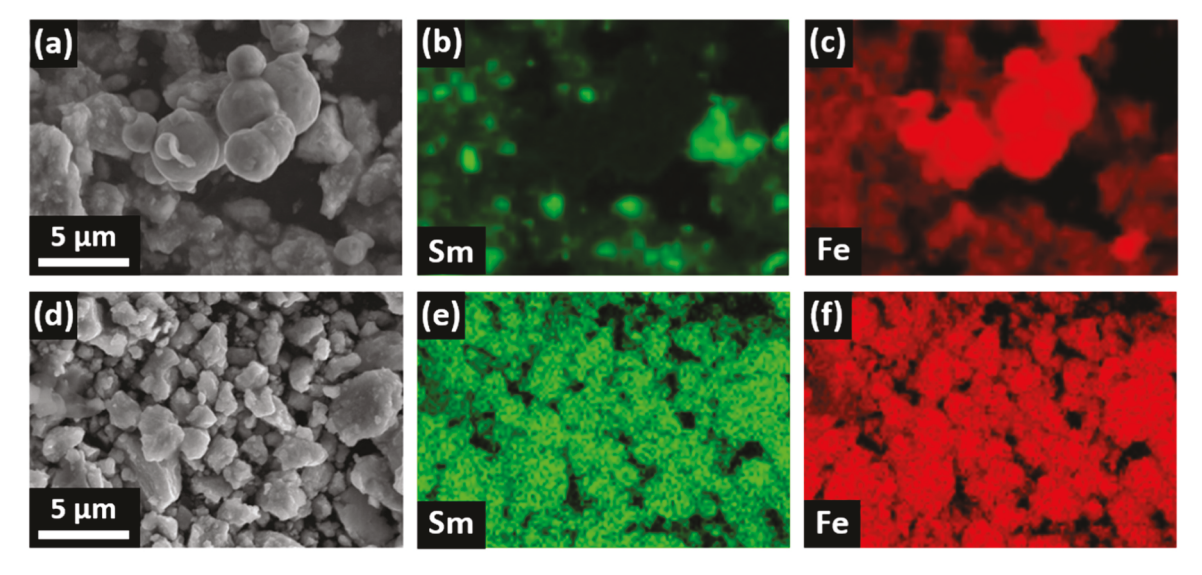


Fig. 2. SEM and EDS mapping images of precursor powders obtained by milling for different times: (a-c) 1 h, and (d-f) 10 h, respectively.

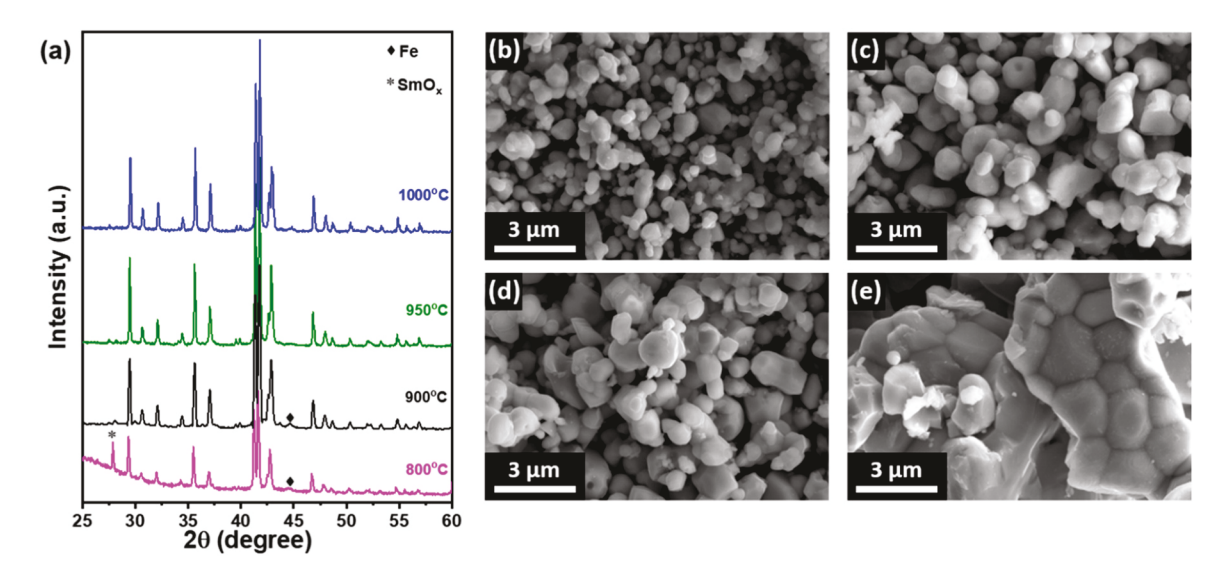


Fig. 3. (a) Powder XRD patterns of Sm₂Fe₁₇N₃ samples prepared at different RD temperatures. (b-d) SEM images of Sm₂Fe₁₇N₃ powders prepared at different RD temperatures (b) 900 °C, (c) 950 °C, (d) 1000 °C respectively, and (e) SEM images of Sm₂Fe₁₇N₃ powders prepared at RD 950 °C without milling and CaCl₂.

3. Results and discussion

The reduction-diffusion (RD) process has been used to obtain Sm₂Fe₁₇N₃ powders and is comprised of mechanochemical activation of precursors, RD, nitriding of obtained materials, and followed by washing out byproducts. The process of ball milling precursors induces a mechanochemical activation, leading to a reduction in the particle size of iron and facilitating the uniform mixing of the precursor materials. During RD at elevated temperatures, Ca metal melts, dissolves in CaCl₂ flux, and diffuses to vicinity of Sm₂O₃. Further, the Sm₂O₃ compound is reduced by molten Ca, forming CaO and Sm metal which diffuses into the Fe particles producing a Sm₂Fe₁₇ compound. Controlling the RD process relies on the structural characteristics of precursor powder particles, such as their shape, size, and homogeneity [21]. The application of mechanical energy, achieved through ball milling (BM), changes particle size and morphology, thus activating the precursors [22]. We conducted a systematic investigation to determine how the morphological modifications in precursor powder particles induced by BM affect the RD products. For this purpose, the precursor mixture was subjected to the BM for various time intervals: 1, 3, 6, and 10 h. The morphological changes of the resulting particles are illustrated in Fig. 1. SEM analysis indicated that milling for 10 h produces particles with more uniform shapes, whereas shorter milling durations results in a variety of particle shapes consisting of spherical and flake shaped particles. Additionally, based on the backscattered electron (BSE) SEM analysis, the presence of high-intensity zones suggest that the precursors are not fully mixed. On the other hand, the 10 h BM sample has a granular morphology without any high-intensity zones indicating uniform mixing. Furthermore, the particles size decreases with the BM time as expected [23].

Fig. 2 presents the EDS elemental mapping for the 1 h and 10 h BM samples to better examine the mixing efficiency and morphological transformations of the precursor powder with the BM time. The sample subjected to 1 h BM (Fig. 2a–c) clearly features isolated Fe and $\rm Sm_2O_3$ particles, implying a shorter BM time does not allow for proper mixing of the precursors. On the other hand, EDS of the 10 h BM sample indicates that Fe and Sm are uniformly distributed (Fig. 2d–f). Therefore, longer milling promotes a uniform mixing of precursors along with the particle size reduction resulting in a granular morphology.

The XRD patterns and morphological changes of Sm₂Fe₁₇N₃

Fig. 4. Schematic diagram illustrating mechanism of Sm-Fe formation via the CaCl2-assisted reduction-diffusion process.

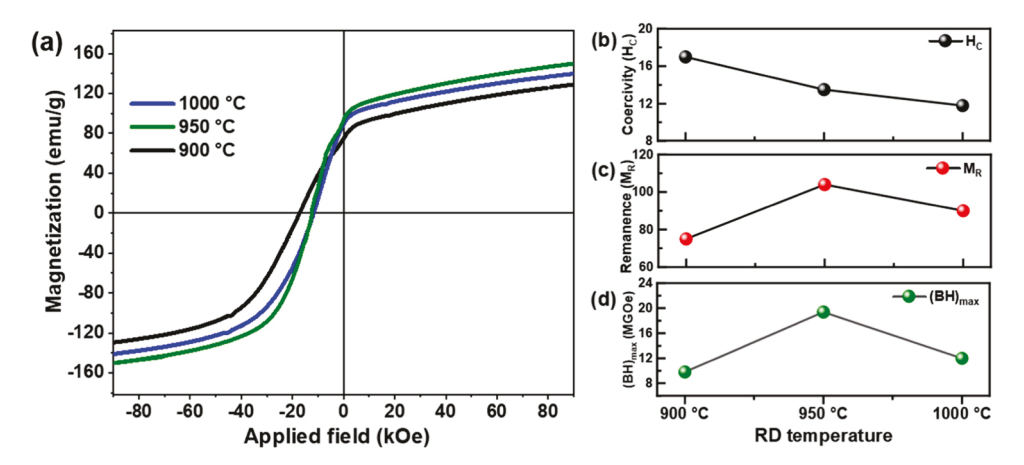


Fig. 5. (a) Room temperature magnetization curves of $Sm_2Fe_{17}N_3$ powders prepared at different RD temperatures, (b–d) H_C , M_R and $(BH)_{max}$ against RD temperatures.

powders, which were obtained by BM for 10 h of precursors, followed by RD process at different temperatures from 800 to 1000 °C, and subsequent nitridation and washing, are shown in Fig. 3a. All the samples have the $Sm_2Fe_{17}N_3$ magnetic phase as a main phase [JCPDS#04-009-7147]. However, after synthesis at 800 °C, along with the major phase $(Sm_2Fe_{17}N_3)$ there are additional impurity phases including unreacted $\alpha\text{-Fe}$ and SmO_x phase. After synthesis at 900 °C, the only impurity present is $\alpha\text{-Fe}$ phase. Due to its nonmagnetic nature, the SmO_x phase reduces overall magnetization and may prevent reaching high relative densities during consolidation process. The soft-magnetic $\alpha\text{-Fe}$ is also detrimental because it serves as nucleation site for the reverse magnetic domains [24]. The samples produced at RD temperatures of 950 °C or higher are single-phase materials, which is expected to favor the high hard-magnetic properties.

The surface morphology for the samples obtained at different RD temperatures is shown in Fig. 3b-e. The particle sizes clearly increase with the RD temperature from $\sim\!1$ to $\sim\!2$ µm. Additionally, particle aggregation is observed especially at elevated RD temperatures. However, the sample prepared without utilizing CaCl $_2$ as a dispersant is highly aggregated as is evident from corresponding SEM image (Fig. 3e). The milling of precursors with CaCl $_2$ likely achieves homogeneous mixing. Subsequently, during RD, the molten CaCl $_2$ acts as a barrier between the Fe particles, preventing excessive sintering, and during washing step due

to its much higher water solubility (compared to CaO), it facilitates liberation of the as formed Sm-Fe particles and CaO by-product, decreasing washing time and consequently surface oxidation.

The proposed mechanism of Sm-Fe formation via the CaCl $_2$ -assisted RD is illustrated in the schematic diagram presented in Fig. 4. Thus, Ca dissolves in molten CaCl $_2$, creating a {Ca+CaCl $_2$ } liquid flux which reduces Sm $_2$ O $_3$, generating Sm metal while producing CaO as a byproduct. The resulting Sm undergoes dissolution in CaCl $_2$ flux, diffuses and reacts with Fe particles resulting in the formation of Sm-Fe alloy. Therefore, the molten CaCl $_2$ plays a crucial role in effectively facilitating diffusion and reaction between Sm and Fe.

Fig. 5 shows the demagnetization curves of samples (aligned under a magnetic field and fixed in a wax) prepared at different RD temperatures. Clearly, the RD temperature significantly affects the hard-magnetic properties of the synthesized materials, as summarized in Table 1. Due to the absence of impurities and low sintering, the sample obtained at 950 °C demonstrates the highest values of magnetization $M_{90}=140$ emu/g, magnetic ratio $M_R/M_{90}=0.74$ with coercivity $H_C=19.4$ kOe. While the sample synthesized at RD temperature of 900 °C exhibited poor hard-magnetic characteristics, namely reduced $M_{90},\,M_R,$ and $(BH)_{max},$ due to the presence of an additional phase (Fig. 3a, black pattern), it also demonstrated higher H_C value – attributed to its smaller particle size. In contrast, the sample obtained at 1000 °C possessed a

Table 1
Hard-magnetic properties of the Sm₂Fe₁₇N₃ powders prepared at different RD temperatures.

| RD temperature | Magnetization at 90 kOe M_{90} (emu/g) | Remanence M _R (emu/g) | Coercivity H _C (kOe) | Magnetic ratio $M_R/M_{\rm 90}$ | Max. energy density (BH) _{max} (MGOe) |
|------------------|--|----------------------------------|---------------------------------|---------------------------------|--|
| 900 °C 950 °C | 126 140 | 75 104 | 17 13.5 | 0.60 0.74 | 9.8 19.4 |
| 1000 °C | 137 | 90 | 11.8 | 0.65 | 12 |

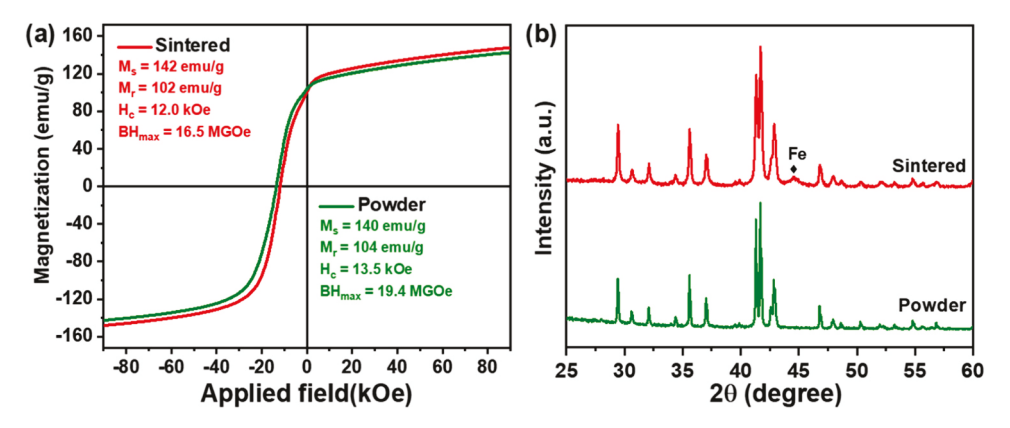


Fig. 6. (a) Room temperature magnetization curves, (b) XRD patterns of Sm₂Fe₁₇N₃ powder and sintered magnet.

markedly lower H_C value compared to all other samples which results from stronger sintering at elevated temperatures. Thus, the best performing powder obtained upon reduction-diffusion at 950 $^{\circ}\text{C}$ after alignment in field and fixing in wax demonstrated maximum energy product BH_{max} of 19.4 MGOe.

The enhanced hard-magnetic properties of obtained samples are related to the single-phase formation, minimal aggregation of magnetic particles, and the precursor powders homogeneous mixing. Thus, BM of precursor powders is necessary to obtain the uniform mixing of all reactants with 10 h BM being an optimal length of time. Particularly, the $\rm Sm_2Fe_{17}N_3$ magnetic particles prepared by 10 h BM of precursor powders followed by 950 °C RD demonstrated higher (BH)_{max} value when compared to the previous reports for $\rm Sm_2Fe_{17}N_3$ magnetic particles synthesized using bottom-up chemical methods [14,15,17,18]. The magnetic properties improvement of the final $\rm Sm_2Fe_{17}N_3$ magnetic particles can be attributed to the uniform particle shape, minimal particle aggregation, high crystallinity, and purity of the hard-magnetic phase [22,25]. Additionally, the BM of the precursor powders with process control agent CaCl₂ facilitates deagglomeration of the magnetic particles on washing increasing both $\rm H_C$ and $\rm M_R/M_{90}$.

To produce a bulk magnet from the synthesized Sm₂Fe₁₇N₃ magnetic powders, the best-performing 950 °C RD powder sample was consolidated using Spark Plasma Sintering (SPS) under 750 MPa at 420 °C, achieving a relative density of 86 % in the process. Notably, the hardmagnetic properties are substantially retained with only a small loss in H_C resulting in (BH)_{max} value of 16.5 MGOe (Fig. 6a). The reason for H_C deterioration in the sintered sample can be attributed to the presence of smaller particles, approximately $1.2 \, \mu m$ in size, which developed a thin amorphous surface oxide layer during the washing step. This resulted in the precipitation of the soft-magnetic α-Fe phase during sintering serving as nucleation sites for the reverse magnetic domains [24]. This is confirmed by the powder XRD phase analysis of the sintered sample (Fig. 6b), which shows a broad low-intensity Fe peak at approximately 45° 20. Due to only small amounts of α -Fe, the hard-magnetic properties of the sintered sample remained consistent with the properties of the powder used for compaction (Fig. 5a). These results indicate that the extent of oxidation of our Sm₂Fe₁₇N₃ magnetic particles is substantially lower when compared with previous reports [9]. Therefore, the developed RD process yields the Sm₂Fe₁₇N₃ powders with improved hard-magnetic properties and lower surface oxidation.

4. Conclusions

 $Sm_2Fe_{17}N_3$ magnetic powders and a bulk magnet were produced using a CaCl2-molten salt-assisted reduction-diffusion (RD) process followed by nitrogenation, washing, and Spark Plasma Sintering (SPS). Incorporating ball milling (BM) of the precursor powders with CaCl2 as a process control agent, mechanochemically activated the precursors and facilitated homogeneous mixing, thus expediting the RD process at

lower temperatures. The sample produced by BM for 10 h and RD at 950 $^{\circ}\text{C}$ exhibited excellent morphological properties and phase purity boosting hard-magnetic properties: (BH)_{max} = 19.4 MGOe and H_C of 13.5 kOe. This excellent hard-magnetic properties were attributed to the less agglomerated particles due to BM and use of CaCl_2 during RD process. Furthermore, the best-performing powder, when subjected to SPS, yielded a sintered magnet with a relative density of 86 % and (BH)_{max} of 16.5 MGOe. Only a small decrease in H_C of a bulk magnet was observed when compared with a powder. Hence, the bottom-up RD process outlined in this study successfully produced the $\text{Sm}_2\text{Fe}_{17}\text{N}_3$ powders exhibiting enhanced hard-magnetic properties and low particle surface oxidation, as confirmed by fabrication of a sintered magnet without significant deterioration of magnetic properties.

CRediT authorship contribution statement

Schlagel Deborah: Data curation, Formal analysis. Thomas A. Seymour-Cozzini: Data curation, Formal analysis. Rambabu Kuchi: Conceptualization, Data curation, Writing – original draft. Julia V. Zaikina: Funding acquisition, Resources. Ihor Z. Hlova: Conceptualization, Project administration, Supervision, Writing – review & editing.

Declaration of Competing Interest

The authors declare that they have no known competing financial interests or personal relationships that could have appeared to influence the work reported in this paper.

Data availability

Data will be made available on request.

Acknowledgements

This work was performed at the Ames National Laboratory and supported by the Critical Materials Innovation Hub funded by the US Department of Energy, Office of Energy Efficiency and Renewable Energy, Advanced Materials and Manufacturing Technologies Office. Ames National Laboratory is operated for the U.S. DOE by Iowa State University under contract DE-AC02–07CH11358. J.V.Z. acknowledges financial support from the National Science Foundation (DMR 1944551 CAREER award).

References

- T. Saito, K. Kikuchi, Production of SmFeN bulk magnets by the spark plasma sintering method with dynamic compression, J. Alloy. Compd. 673 (2016) 195–198.
- [2] W. Li, Research progress of SmFeN rare-earth permanent magnet, Mater. Sci. 11 (2021) 649–664.

- [3] V. Galkin, R. Kuchi, S. Kim, J.R. Jeong, T. Kim, Y. Baek, D. Kim, Nd-Fe-B particles with reduced oxygen content and enhanced magnetic properties prepared through reduction-diffusion and novel washing process, J. Magn. Magn. Mater. 578 (2023) 170822
- [4] P.E. Kakosimos, A.G. Sarigiannidis, M.E. Beniakar, A.G. Kladas, C. Gerada, Induction motors versus permanent-magnet actuators for aerospace applications, IEEE Trans. Ind. Electron. 61 (2014) 4315–4325.
- [5] S. Okada, K. Suzuki, E. Node, K. Takagi, K. Ozaki, Y. Enokido, Preparation of submicron-sized Sm2Fe17N3 fine powder with high coercivity by reductiondiffusion process, J. Alloy. Compd. 695 (2017) 1617–1623.
- [6] J.M.D. Coey, H. Sun, Improved magnetic properties by treatment of iron-based rare earth intermetallic compounds in anmonia, J. Magn. Magn. Mater. 87 (1990) 1251-1254
- [7] L. Zhao, N.G. Akadogan, G.C. Hadjipanayis, Hard magnetic Sm2Fe17N3 flakes nitrogenized at lower temperature, J. Alloy. Compd. 554 (2013) 147–149.
- [8] J.J. Wysłocki, P. Pawlik, W. Kaszuwara, M. Leonowicz, Magnetic properties and intrinsic magnetic parameters of nanocrystalline Sm-Fe-N magnets, J. Magn. Magn. Mater. 272 (2004) 1929–1930.
- [9] R. Soda, K. Takagi, M. Jinno, W. Yamaguchi, K. Ozaki, Anisotropic Sm2Fe17N3 sintered magnets without coercivity deterioration, AIP Adv. 6 (2016) 115108.
- [10] D. Liang, W. Yang, X. Wang, Q. Xu, J. Han, S. Liu, C. Wang, H. Du, X. Zhu, T. Yuan, Z. Luo, J. Yang, Study of the anisotropic Sm2Fe17N3 powders with high performance, AIP Adv. 13 (2023) 025104.
- [11] M. Xing, J. Han, F. Wan, S. Liu, C. Wang, J. Yang, Y. Yang, Preparation of anisotropic Sm2Fe17N3 magnetic materials by strip casting technique, IEEE Trans. Magn. 49 (2013) 3248–3250.
- [12] M. Xing, J. Han, Y. Zhang, S. Liu, Z. Chen, C. Wang, J. Yang, H. Du, Y. Yang, M. Yue, Nitrogenation effect of Sm2Fe17 alloys prepared by strip casting technique, J. Appl. Phys. 117 (2015) 17A732.
- [13] A. Kawamoto, T. Ishikawa, S. Yasuda, K. Takeya, K. Ishizaka, T. Iseki, K. Ohmori, Sm2Fe17N3 magnet powder made by reduction and diffusion method, IEEE Trans. Magn. 35 (2012) 3322.
- [14] S. Okada, K. Takagi, K. Ozaki, Investigation of optimal route to fabricate submicron-sized Sm2Fe17 particles with reduction-diffusion method, AIP Adv. 6 (5) (2016) 056018.

- [15] S. Okada, K. Takagi, K. Ozaki, Direct preparation of submicron-sized Sm2Fe17 ultra-fine powders by reduction-diffusion technique, J. Alloy. Compd. 663 (2016) 872.
- [16] S. Okada, E. Node, K. Takagi, Y. Fujikawa, Y. Enokido, C. Moriyoshi, Y. Kuroiwa, Synthesis of Sm2Pe17N3 powder having a new level of high coercivity by preventing decrease of coercivity in washing step of reduction-diffusion process, J. Alloy. Compd. 804 (2019) 237–242.
- [17] J. Zheng, S. Tian, K. Liu, W. Cai, Y. Tang, L. Qiao, Y. Ying, W. Li, J. Yu, Y. Liu, S. Che, Preparation of submicron-sized Sm2Fe17N3 fine powder by ultrasonic spray pyrolysis-hydrogen reduction (USP-HR) and subsequent reduction-diffusion process, AIP Adv. 10 (2020) 055119.
- [18] J. Lee, E. Lee, K. Koo, M. Kang, H. Lee, M. Lim, J. Kim, Y. Choa, One-pot synthesis and large-scale production strategies for preparing ultrafine hard magnetic Sm2Fe17N3 nanoparticles, ACS Appl. Nano Mater. 5 (2022) 176–182.
- [19] S. Sato, K. Nishikawa, E. Node, S. Okada, Development of TbCu7-type Sm-Fe-N anisotropic magnet powder and its sintered magnets, J. Alloy. Compd. 929 (2022) 167280.
- [20] T. Iriyama, K. Kobayashi, N. Imaoka, T. Fukuda, H. Kato, Y. Nakagawa, Effect of nitrogen content on magnetic properties of Sm2Fe17Nx (O<x<6), IEEE Trans. Magn. 28 (1992) 2326–2331.
- [21] R.K. Sidhu, Influence of particle size of iron powder on the microstructure of Nd–Fe–B alloy powder prepared by reduction-diffusion, J. Alloy. Compd. 346 (2002) 250–254.
- [22] R. Kuchi, V. Galkin, S. Kim, J.-R. Jeong, S. Hong, D. Kim, Synthesis of NdFeB magnetic particles with high (BH)max from their optimized oxide powders through reduction-diffusion method, IEEE Magn. Lett. 13 (2022) 7504004.
- [23] D. Shin, B. Madavali, D. Kim, J.Y. Lee, M. Kang, C. Yang, C. Suryanarayana, S. J. Hong, Investigation of the magnetic properties and fracture behavior of Nd–Fe–B alloy powders during high-energy ball milling, Mater. Res. Exp. 7 (2020) 096101.
- [24] W. Yamaguchi, R. Soda, K. Takagi, Role of surface iron oxide in coercivity deterioration of Sm2Fe17N3 magnet associated with low temperature sintering, Mater. Trans. 60 (2019) 479–483.
- [25] S. Kim, V. Galkin, J.R. Jeong, R. Kuchi, D. Kim, Enhanced magnetic and structural properties of chemically prepared Nd-Fe-B particles by reduction-diffusion method through optimization of heat treatments, J. Alloy. Compd. 869 (2021) 159337.